Solution conformation on bovine growth hormone releasing factor by ^{1}H NMR and molecular modeling

Jeehye Kweon[a], Ho-Jin Lee[a], Young-Man Kim[a], Young-Sang Choi[b], Kang-Bong Lee[a,*]

[a] *Advanced Analysis Center, Korea Institute of Science and Technology, P.O. Box 131, Cheongryangri, Seoul 130-650, South Korea*
[b] *Department of Chemistry, Korea University, Seongbukku, Anamdong, Seoul 136-701, South Korea*

Received 16 April 1999; received in revised form 29 June 1999

Abstract The structure of bovine growth hormone releasing factor (bGHRF) consisting of 44 amino acids has been studied in CD and ^{1}H nuclear magnetic resonance (NMR) spectroscopy in conjunction with molecular modeling. Since bGHRF does not have an ordered structure in water alone, a 30% 2,2,2-trifluoroethanol (TFE) aqueous solvent was used to induce considerable α-helical structures, which corresponds to a helical content of ∼62% as determined by circular dichroism (CD). The secondary structure was obtained from nuclear Overhauser enhancement and $^3J_{HN\alpha}$ coupling constant in 30% TFE solution. Three-dimensional structures consistent with NMR data were generated by using distance geometry calculation. A set of 267 interproton distances derived from nuclear Overhauser effect correlation spectroscopy (NOESY) experiments and coupling constants were used. From the initial random conformations, 50 distance geometry structures with minimal violations were selected for further refinement. The 14 best structures were obtained after simulated annealing calculation with energy minimization. The structure of bGHRF in 30% TFE solution was characterized by one α-helix (residues 8–19), two poorly constrained helices (residues 23–27 and residues 31–34) and a β I(III)-turn fragment (residues 20–23; $\phi_{i+1} = -53.1°$, $\Psi_{i+1} = -19.6°$, $\phi_{i+2} = -59.9°$, $\Psi_{i+2} = -20.6°$) connected by the segments of less defined structures in N-terminal and Ω-shaped flexible C-terminal determined from NOESY cross peaks between helical segment (residues 14–18) and tail fragment (residues 42–44). The obtained structure will play an important role toward the understanding of the structural and functional role of the GHRF.

Key words: Growth hormone releasing factor; CD; NMR; Three-dimensional structure; Distance geometry; Restrained molecular dynamics

1. Introduction

The growth hormone releasing factor (GHRF) is a polypeptide hormone consisting of 44 amino acids which stimulate the secretion of growth hormone in vivo of all vertebrates [1]. The functional studies on GHRF have been performed to characterize this peptide's role in the control of growth hormone secretion and human GHRF has been used clinically as an alternative to growth hormone therapy for growth hormone deficient children [2]. Since structure-activity studies have shown that the shortened sequence GHRF(1–29)NH_2 retains almost complete biological activity relative to full sequences both in vivo and in vitro [3–5], the structures of GHRF(1–29)NH_2 and GHRF analogues rather than full sequence have been deduced from a combined circular dichroism and nuclear magnetic resonance (NMR) study [6–10]. The secondary structure of human ^{27}Nle-GHRF(1–29)NH_2 has been determined as extended conformations consisting of a short β-strand and two α-helices connected by short segments of less well defined secondary structure [8]. Despite the considerable effort to physiological and structural aspects in GHRF, its full sequence structure in solution and single crystal has not been characterized. The primary structures of peptides with high intrinsic growth hormone releasing activity have been established from four different species as shown in Fig. 1. Human, porcine and bovine sequences possess a carboxyl terminally amidated 44 amino acid structure, but rat GHRF containing only 43 amino acids is not amidated. As a first step to characterize the three-dimensional structure of GHRF full sequence (1–44) peptide, we synthesized the full sequence of bovine GHRF (bGHRF).

We present the three-dimensional solution structure of bGHRF full sequence (1–44) peptide using nuclear magnetic resonance (NMR) data in conjunction with distance geometry and restrained molecular dynamics (MD). The determination of the three-dimensional structure on bGHRF by NMR spectroscopy was proceeded in three stages; (1) the sequential assignment of resonances by means of through-bond and through-space connectivity [11]; (2) the derivation of an approximate set of interproton distances from the nuclear Overhauser enhancement (NOE) data and dihedral angles [12]; and (3) the determination of the three-dimensional structure by performing distance geometry and a MD simulation on the basis of NOE distances [13]. The obtained conformation should satisfy the constraints. If there is good agreement with all NMR parameters, the conformation is assumed to represent the solution conformation.

The information of the precise tertiary structure on bGHRF will shed light on probing this peptide's role as well as appropriate direction for the design of the simple lead compound with the same activity in comparison to GHRF.

2. Materials and methods

2.1. Peptide synthesis

The peptide, bGHRF was synthesized by standard solid phase syn-

*Corresponding author. Fax: (82) (2) 958-5969.
E-mail: leekb@kistmail.kist.re.kr

Abbreviations: TFE, 2,2,2-trifluoroethanol; DIANA, distance geometry algorithm for NMR applications; DQFCOSY, double quantum filtered correlation spectroscopy; DSA, dynamical simulated annealing; bGHRF, bovine growth hormone releasing factor; MD, molecular dynamics; NMR, nuclear magnetic resonance; NOESY, nuclear Overhauser effect correlation spectroscopy; RMSD, root mean square deviation; TOCSY, total correlation spectroscopy; CD, circular dichroism

0014-5793/99/$20.00
PII: S0014-5793(99)00976-X

thesis methods [14] and purified by high-performance liquid chromatography (HPLC) with trifluoroacetic acid and a linear acetonitrile/water gradient elution on a C_{18} reverse phase column. The purified peptide was characterized by IonSpray MS([MH]$^+$ found = 5107.6; calc. = 5108.8) and by different analytical HPLC conditions (RP C_{18}, Vydac C_{18} and Hichrom C_{18} columns). Amino acid analysis, after acid hydrolysis, gave the correct molar ratios of the constituent acids.

2.2. Circular dichroism experiment

Samples for circular dichroism (CD) spectroscopy contained 0.24 mg peptide/ml in water varying amounts of 2,2,2-trifluoroethanol (TFE) and temperature at pH 3.5. CD spectra were recorded from 180 nm to 250 nm on a JASCO J-715 spectropolarimeter equipped with NEC pc-9801 computer. Cells with 1 mm pathlength were used and the spectra are the averages of five scans. The α-helicity was calculated by using the mean residue ellipticity at 220 nm [θ_{220}] and the equation of Chen et al. [15]: $[\theta]_\lambda = (f_H - 2.6i/N)[\theta]_{H\lambda\infty}$ where $[\theta]_\lambda$ is the observed mean residue ellipticity at wavelength λ, $[\theta]_{H\lambda\infty}$ is the maximum mean residue ellipticity of a helix of a infinite length, f_H is the fraction of helix in the molecule, i is the number of helical segments, N is the total number of residues. Changes in either salt or peptide concentration did not affect the resulting CD spectra in the 30% TFE aqueous solution.

2.3. NMR experiments

All NMR experiments were performed using a 5 mm indirect probe on Varian Unity Plus 600 NMR spectrometer operating at a ^{1}H frequency of 599.945 MHz. The peptide sample (12.5 mg) was dissolved in 20 mM KCl and 50 mM potassium phosphate before TFE-d_3 was added to yield an aqueous 30% (v/v) TFE-d_3 solution. The pH was adjusted by the addition of small amounts of 0.2 M ^{2}HCl or 0.2 M NaO^{2}H and was measured using a Beckman model F34 pH meter equipped with an Ingold microcombination electrode; pH values were not corrected for the isotope effect. One-dimensional NMR spectra and two-dimensional COSY, double quantum filtered correlation spectroscopy (DQFCOSY), total correlation spectroscopy (TOCSY) and nuclear Overhauser effect correlation spectroscopy (NOESY) were acquired with a pre-saturation delay of 1.5 s. TOCSY spectrum was recorded using a WALTZ-17 spin-lock pulse sequence with 150 ms mixing time. The NOESY data were acquired with 50, 100, 200 and 300 ms mixing times. Usually 256×4096 data points were collected and for each blocks 128 scans were collected for two-dimensional experiments. The data set were linearly predicted to 1024×4096 data points. A Gaussian and Sinbell windows was applied in both dimensions. Zero filling was used to bring the final spectrum size to 4096×4096 data points. The chemical shifts were referenced to sodium 4,4-dimethyl-4-silapentane-1-sulfonate (DSS, 0.0 ppm).

Table 1
^{1}H chemical shift values for bGHRF in 30% TFE aqueous solution from F2 dimension at pH = 3.5, 20°C

Residue	NH	C_αH	C_βH	Others (ppm)
Y1	–	4.24	3.14, 3.24	^{2,6}H 7.22 ^{3,5}H 6.94
A2	8.47	4.36	1.42	
D3	8.34	4.23	2.89, 3.25	
A4	8.34	4.23	1.46	
I5	7.81	3.95	1.91	γ-CH_2 1.19, 1.46 γ-CH_3 0.81 δ-CH_3 0.87
F6	7.96	4.48	3.19, 3.24	^{2,6}H 7.28 ^{3,5}H 7.21 ^{4}H 7.30
T7	8.17	4.09	4.34	γ-CH_3 1.34
N8	8.31	4.61	2.84, 2,98	γ-NH_2 6.93, 7.60
S9	8.09	4.31	3.93, 4.02	
Y10	8.22	4.28	2.95, 2.99	^{2,6}H 7.04 ^{3,5}H 6.82
R11	8.04	3.92	1.88, 1.98	γ-CH_2 1.69 δ-CH_2 3.25 NH 7.18
K12	7.81	4.09	2.04	γ-CH_2 1.55 δ-CH_2 1.63 ε-CH_2 3.07 ε-NH_3 7.45
V13	7.86	3.73	2.22	γ-CH_3 0.98, 1.09
L14	8.36	4.08	1.63, 1.72	γ-CH 1.57 δ-CH_3 0.84
G15	8.31	3.96		
Q16	7.94	4.21	2.35	γ-CH_2 2.45, 2.57 δ-NH_2 6.71, 7.25
L17	7.99	4.24	1.58	γ-CH 1.58 δ-CH_3 0.96, 1.00
S18	8.09	4.31	4.02	
A19	7.88	4.19	1.56	
R20	7.98	4.05	1.87,2.05	γ-CH_2 1.77 δ-CH_2 3.20 NH 7.29
K21	8.10	4.13	1.78, 2.04	γ-CH_2 1.49 δ-CH_2 1.67 ε-CH_2 3.02 ε-NH_3 7.45
L22	8.04	4.40	1.70	γ-CH 1.70 δ-CH_3 0.90, 0.96
L23	8.27	4.11	1.83	γ-CH 1.81 δ-CH_3 0.93, 0.96
Q24	8.19	4.01	2.27, 2.42	γ-CH_2 2.58 δ-NH_2 6.75, 7.36
D25	8.34	4.53	2.93, 3.25	
I26	8.60	3.72	2.09	γ-CH_2 1.90, 1.13 γ-CH_3 0.97 δ-CH_3 0.90
M27	8.68	4.24	2.15, 2.27	γ-CH_2 2.62, 2.82 ε-CH_3 2.27
N28	8.58	4.59	2.93, 3.10	γ-NH_2 6.85, 7.60
R29	8.09	4.45	1.80, 1.92	γ-CH_2 1.71 δ-CH_2 3.26 NH 7.23
Q30	8.38	4.20	2.23	γ-CH_2 2.54 δ-NH_2 6.78, 7.40
Q31	8.28	4.18	2.22	γ-CH_2 2.48 δ-NH_2 6.62, 7.08
G32	8.14	3.99	2.25	
E33	8.43	4.17	2.24	γ-CH_2 2.45, 2.60
R34	8.14	4.23	1.82, 1.96	γ-CH_2 1.72 δ-CH_2 3.22 NH 7.26
N35	8.31	4.71	2.92	γ-NH_2 6.88, 7.72
Q36	8.30	4.44	2.10, 2.22	γ-CH_2 2.43 δ-NH_2 6.79, 7.45
E37	8.14	4.30	2.21	γ-CH_2 2.51, 2.60
Q38	8.24	4.37	2.10, 2.22	γ-CH_2 2.43 δ-NH_2 6.75, 7.44
G39	8.24	3.98		
A40	7.95	4.34	1.49	
K41	8.08	4.35	1.85, 1.92	γ-CH_2 1.56 δ-CH_2 1.75 ε-CH_2 3.05 ε-NH_3 7.45
V42	7.80	4.15	2.13	γ-CH_3 0.99, 1.09
R43	8.19	4.20	1.87, 2.03	γ-CH_2 1.74 δ-CH_2 3.23 NH 7.28
L44	8.60	4.13	1.92	γ-CH 1.90 δ-CH_3 0.90, 0.95

```
          1         5         10        15        20        25        30        35        40
bGHRF  Y A D A I F T N S Y R K V L G Q L S A R K L L Q D I M N R Q Q G E R N Q E Q G A K V R L
pGHRF  Y A D A I F T N S Y R K V L G Q L S A R K L L Q D I M S R Q Q G E R N Q E Q G A R V R L
hGHRF  Y A D A I F T N S Y R K V L G Q L S A R K L L Q D I M S R Q Q G E S N Q E Q G A R A R L
rGHRF  H A D A I F T S S Y R R I L G Q L Y A R K L L H E I M N R Q Q G E R N Q E Q R S R F N
```

Fig. 1. Primary structures of the bovine, human, pig and rat GHRF.

2.4. Molecular modeling

Structure calculations were carried out using the Tripos molecular modeling software SYBYL (ver. 6.3) [16]. The NOESY data acquired with a mixing time of 200 ms were used to derive the interproton distances. Although spin diffusions were not found from major cross peaks of 300 ms mixing time NOESY data, we did not consider it due to the possibility for spin diffusion. For upper and lower distance bounds an additional harmonic function was employed. The function switches from harmonic to linear when the deviation is greater than 10% of the target distance. The medium and long range NOEs have maximum limit value 4.0 and 5.0 Å upper bound, respectively. Standard pseudoatom corrections were added, if necessary [13].

The distance geometry program: distance geometry algorithm for NMR applications (DIANA) [17] was used to generate the starting structure utilizing the redundant dihedral angle constraints (REDAC) strategy [18]. The 267 distance constraints obtained from NOESY cross-peak volumes and seven torsional angle constraints were used for structure calculation. The 200 initial structures randomly generated in the (ϕ, Ψ) space. The best 50 conformers were selected by Widmer et al.'s proposed method [19]. Each conformer was refined using a dynamical simulated annealing (DSA) protocol [20]. One cycle of heating and cooling was applied to each conformer with a time step of 1.0 fs for the integration of Newton's equation of motion (Verlet algorithm) for a duration of 7 ps.

The force constants for upper and lower boundaries were initially set at 20 kcal/mol Å^2. The atomic velocities were applied following a Boltzmann distribution about center of mass to obtain a starting temperature of 700 K. After simulating for 2 ps at this high temperature, the system temperature was exponentially reduced over 5 ps period to reach a final temperature of 200 K.

Resulting structures were minimized to 500 steps by the conjugate gradient algorithm: termination criterium is gradient 0.05 kcal/mol Å^2, stored in a separate database. Before energy minimization was applied to these structures, the force constants of the distance range constraint were set to a lower value of 3 kcal/mol Å^2 to allow the molecule to relax from the strain imposed by experimentally derived constraints.

The β-turn is defined for four consecutive residues (denoted by ϕ_{i+1}, Ψ_{i+1}, ϕ_{i+2}, Ψ_{i+2}) and the β I(III)-turn is assigned on the basis of $\phi_{i+1} = -60°$, $\Psi_{i+1} = -30°$, $\phi_{i+2} = -90°$, $\Psi_{i+2} = -0°$, which are allowed to vary ± 30° from these ideal values with the added flexibility of one angle. The β I(III)-turn in four consecutive residues was determined from the average of the best structures of bGHRF obtained from DIANA and simulated annealing (MD) with restrained energy minimization.

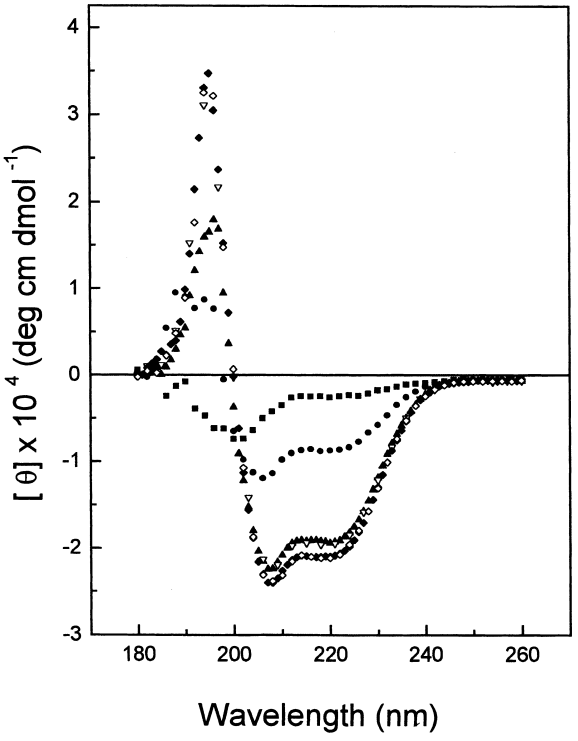

Fig. 2. CD spectra of the bGHRF with various TFE concentration in aqueous solution at 20°C: (■) 0%, (●) 10%, (▲) 20%, (▽) 30%,(◆) 40% (◇) 50% TFE aqueous solution. The helicity from CD data was calculated according to the equation described in text; $f_H = 7.9\%$ at 0% TFE; $f_H = 27.8\%$ at 10% TFE; $f_H = 61.7\%$ at 20% TFE; $f_H = 61.9\%$ at 30% TFE; $f_H = 66.6\%$ at 40% TFE; $f_H = 66.8\%$ at 50% TFE concentrations, respectively.

3. Results and discussion

Fig. 2 shows the far ultraviolet CD spectrum of 78 μM bGHRF in aqueous solution, containing varying amounts of TFE at 20°C and pH 3.5. Upon increasing the TFE concentration there is a significant increase in helical contents as evidenced by the appearance of the distinctive high intensity

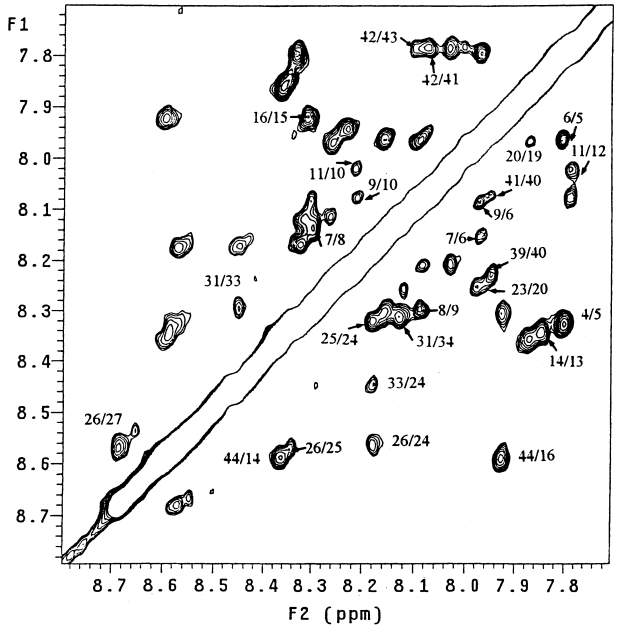

Fig. 3. Amide region of the NOESY spectrum of the bGHRF in 30% TFE aqueous solution at 20°C and pH 3.5. Each peak is numbering to both sides of the residue.

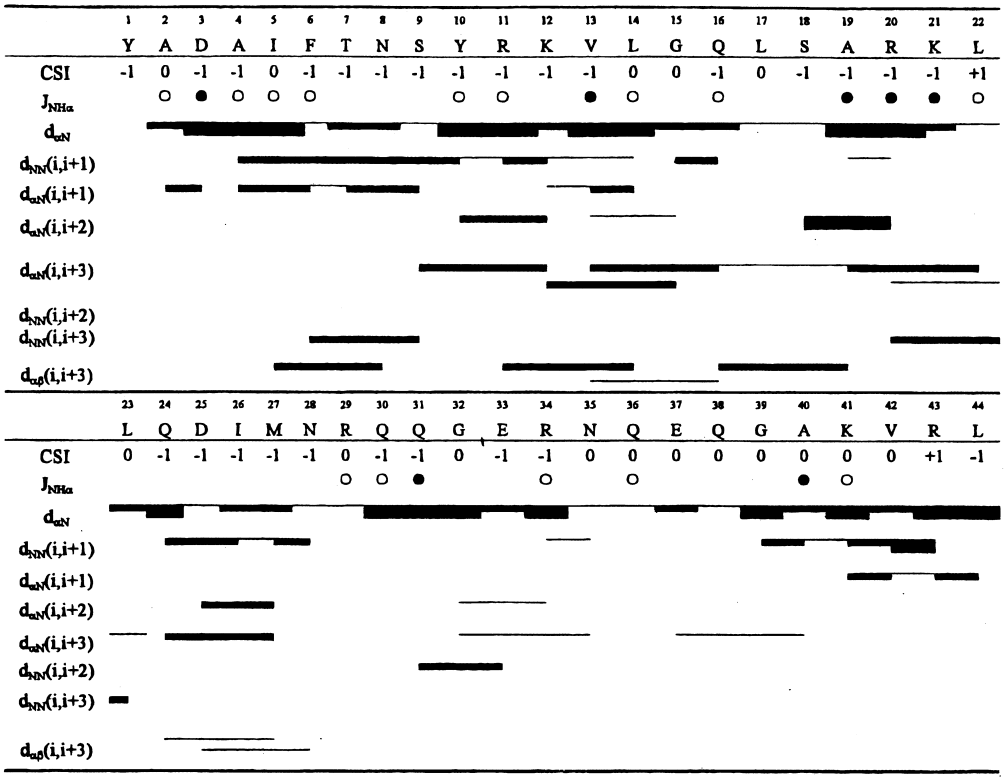

Fig. 4. Intra- and inter-residual NOE connectivities observed for bGHRF with mixing time 200 ms in 30% TFE aqueous solution at 20°C and pH 3.5. NOEs are classified three types: 2.8 Å (strong, filled rectangle), 3.6 Å (medium, thick bar), 5.0 Å (weak, thin bar). The coupling constants symbols: (●) $^3J_{NH\alpha} < 6.0$ Hz, (○) 6.0 Hz $< {}^3J_{NH\alpha} < 7.5$ Hz. Chemical shift index (CSI) of bGHRF in 30% TFE aqueous solution. Any consecutive four or more '−1' and '+1' indices are interpreted as a helix and β conformer, respectively. Other regions are regarded as coil.

band at 222 nm. The transition itself is almost complete at ∼30% concentration of TFE and the maximum value is −19 224.8 deg cm^2/dmol with little dependence on temperatures (5∼25°C). It is shown that although bGHRF does not have an ordered structure in water alone, an aqueous TFE solvent induce considerable α-helical structure of full sequence bGHRF as shown in human ^{27}Nle-GHRF(1–29)NH_2 and full sequence GHRF [7] and this corresponds to a helical content of ∼62% in 30% TFE aqueous solution according to the equation described earlier [15].

The bGHRF displayed well resolved, sharp NMR signals in 30% TFE-d_3 aqueous solution. The ^{1}H one-dimensional and COSY, DQFCOSY, TOCSY and NOESY two-dimensional spectra were obtained as described. The signal assignments were performed with a standard method [13]. The first step was spin system identification which was determined by COSY and TOCSY data recorded in 30% TFE-d_3 aqueous solution at 293 K and pH 3.5. All spin systems were identified using TOCSY at several mixing times in order to record spectra exhibiting single or multiple through-bond connectivities (not shown). Through-space connectivities, of which the inter-residue $C_\alpha H(i)-NH(i+1)$, $NH(i)-NH(i+1)$ and $C_\square H(i)-NH(i+3)$ connectivities are the most important part for the purpose of sequential assignment, were identified by means of NOESY experiments, an example of which is shown in Fig. 3. The certain superimposed resonances of the $NH(i)-NH(j)$ connectivities such as D3/A4, R34/E37 and S8/S18 were assigned by additional NMR experiments at various temperatures (5∼35°C, not shown). Chemical shifts of identified protons are listed in Table 1. The observed NOEs involving the NH, $C_\alpha H$ and $C_\beta H$ classified as strong, medium and weak as well as the $^3J_{NH\alpha}$ coupling constants are summarized in Fig. 4. Evidence of secondary structure was obtained from inter-residue connectivities observed in the NOESY spectrum. $C_\alpha H$ chemical shifts experienced an upfield shift when they are located in a helical segment [21,22]. The difference between $C_\alpha H$ chemical shifts relative to random coil residue $C_\alpha H$ chemical shifts were also displayed in Fig. 4 as the chemical shift index. This chemical shift index and inter-residue NOE connectivities suggests that the fragment Y1-I5 and R29-L44 exist in a fast conformational equilibrium state and the region from F6 to N28 showed an α-helical character as shown in human ^{27}Nle-GHRF(1–29)NH_2 [7]

In the NOESY spectra 267 NOE cross peaks were assigned and these numbers of NOEs led to determine the structure of the peptide using the NOE-derived distance in restrained MD calculations to support the qualitative interpretation of the CD and NMR results and possibly obtain more information about the non-helical regions of the peptide. Distance constraints were derived from the 200 ms mixing time NOESY spectra at 293 K. The interproton distances comprised 162 intra-residue and 105 inter-residue distances. As internal standards, we used the cross peaks between the H_2/ H_6 and H_3/H_5 protons of Y10 ($r = 2.5$ Å). The distances were then calibrated by the method described previously [23] and averaged from both dimensions.

Dihedral angle restraints were additional parameters to supplement NOE restraints. The 29 dihedral angle restraints were derived from $^3J_{HN\alpha}$ coupling constants [24–26], measured by one-dimensional and DQF-COSY in 30% TFE aqueous sol-

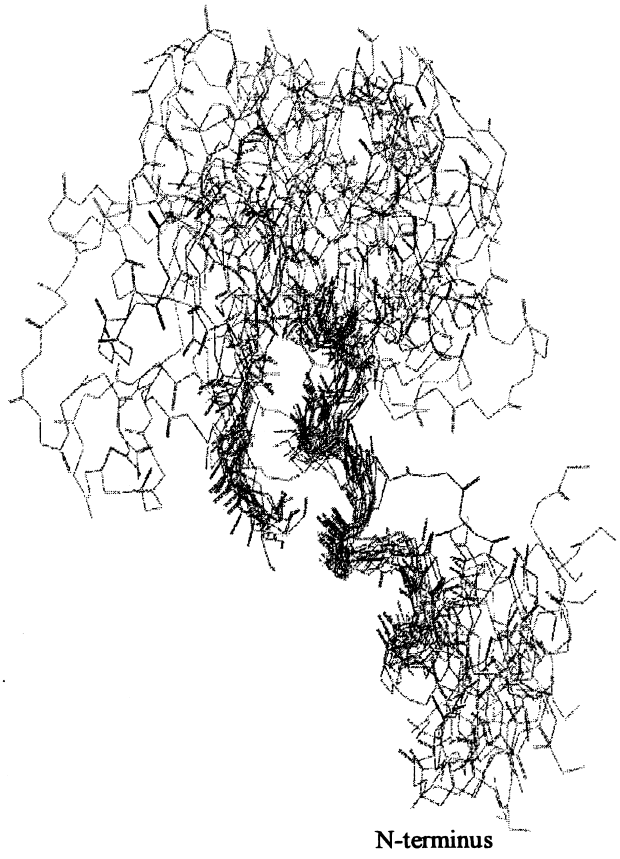

Fig. 5. Superimposition of 14 solution structures of the bGHRF based on the NOE and coupling constant data. The superimposition is shown as a best fit of the backbone for residues 8–19.

ution, but only seven dihedral angle constraints ($^3J_{HN\alpha} \leq 6.0$ Hz) were utilized. The coupling constants suggested that the peptide did not form a very well-defined three-dimensional structure, which indicated that they are usually more flexible and may have more than one preferred conformation. Therefore, the data acquired by NMR will be an average structure of all the conformations existing in the time period of acquisition.

The three-dimensional structure of bGHRF in this solution was constructed using the variable target function software DIANA with its supporting program [17,18]. The input for the present distance geometry calculations of the solution conformation of bGHRF consisted exclusively of geometric constraints determined by NMR experiments and imposed by the primary structure of the proteins. The search for spatial molecular structures compatible with these constraints started without any additional assumptions on the structure to be found, nor was an assumption made as to the existence of a single unique solution [27,28]. The selection of 'good' structures for further analysis from the ensemble (200 structures) generated by DIANA can be based only on the overall distribution of target function, which is a very subjective criteria for defining representative structures. However, more general and unambiguous means of selection structure was implemented [19,29,30], which is based on the maximum values of pairwise root mean square deviations (RMSDs between structures. The 50 good structures were selected from DG

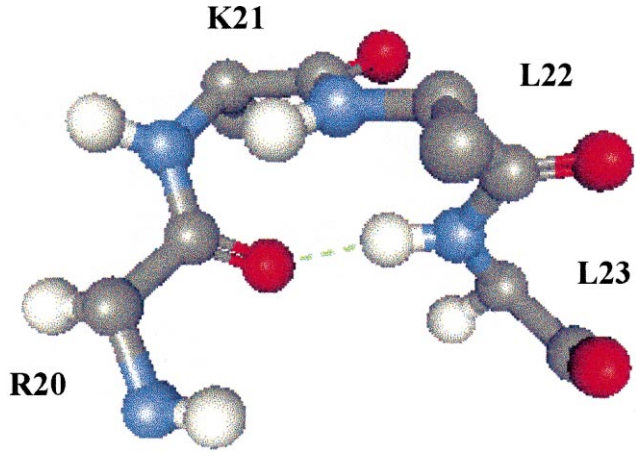

Fig. 6. Stereoview of the minimized mean structure of 14 superimposed structures in residues 20–23, which appears to be a β I(III)-turn fragment ($\phi_{i+1} = -53.1°$, $\Psi_{i+1} = -19.6°$, $\phi_{i+2} = -59.9°$, $\Psi_{i+2} = -20.6°$).

program, which have no violations of upper and lower bounds of NMR distance restraints greater than 0.5 Å, respectively. Fig. 5 presents a superimposition of the polypeptide backbone for 14 best structures of bGHRF(1–44) obtained from DIANA and simulated annealing (MD) with restrained energy minimization. Quantitative character of the 14 DIANA conformers used to present the solution structure of bGHRF is shown in Table 2. The bGHRF conformers obtained from different computation with the same geometric constraints are therefore to be regarded as a random selection from the ensemble of all conformation of the GHRF which are consistent with the experimental data. The average RMSDs between the 14 best structure pairs is 1.24 ± 0.38 Å for backbone atoms and 2.18 ± 1.01 Å for all heavy atoms in residues 8–19, which is shown as a best fit of the backbone for residues 8–19. These structures clearly revealed the α-helical character between residues 8 and 19.

The β-turn is defined for four consecutive residues denoted by ϕ_{i+1}, Ψ_{i+1}, ϕ_{i+2}, Ψ_{i+2} and the β I(III)-turn is assigned on the basis of $\phi_{i+1} = -60°$, $\Psi_{i+1} = -30°$, $\phi_{i+2} = -90°$, $\Psi_{i+2} = -0°$, which are allowed to vary ± 30° from these ideal values with the added flexibility of one angle. The β I(III)-turn in four consecutive residues was determined from the average of the best structures of bGHRF obtained from DIANA and simulated annealing (MD) with restrained energy minimization. A systematic modeling study indicates that an average structure

Table 2
Quantitative character of the 14 DIANA conformers used to present the solution structure of bGHRF

Quantity	Averaged value ± S.D.	Range
Target function (Å^2)	3.64 ± 0.54	(2.55 ~ 4.59)
NOE distance constraint violations		
Sum (Å)	5.0 ± 1.0	(3.2 ~ 6.7)
Maximum (Å)	0.47 ± 0.04	(0.41 ~ 0.57)
Van der Waals violations		
Sum (Å)	1.4 ± 0.5	(0.7 ~ 2.4)
Maximum (Å)	0.31 ± 0.06	(0.25 ~ 0.43)
Torsion angle violation		
Sum (degrees)	3.1 ± 0.8	(1.6 ~ 4.7)
Maximum (degrees)	1.9 ± 0.6	(0.8 ~ 2.9)

in residues 20–23 appears to be a β I(III)-turn fragment (residues 20–23; $\phi_{i+1} = -53.1°$, $\Psi_{i+1} = -19.6°$, $\phi_{i+2} = -59.9°$, $\Psi_{i+2} = -20.6°$) [31] as shown in Fig. 6. The β-turns found in bioactive peptides and proteins serve as a recognizing site for the initiation of biological events [32], and this β I(III)-turn segment seems to be a recognition site for the receptor binding. This fact was partly proved by binding affinity assay using human GHRF(1–29)NH_2 with specifically deleted residues [33]. Although secondary structure by inter-residue NOE connectivities and chemical shift index displayed that three regions (residues 8–19, 23–27 and 31–34) adopted α-helical propensities, our modeling studies revealed the undefined structural features in the N-terminal (residues 1–8) and C-terminal part (residues 20–44). This structural difference may indicate that the residues 23–27 and 31–34 are poorly defined helices in comparison to the segment 8–19. Although C-terminal region exists in random conformation, region 41–44 fold back nearby residues 14–16, which forms Ω-shape loop in the C-terminal. The existence of flexible Ω-shape loop is evidenced from NOESY cross peaks between 44L NH and 16Q $C_\alpha H$, 44L NH and 16Q NH, 44L NH and 14L $C_\alpha H$, 44L NH and 14L NH, and 42V NH and 18S $C_\alpha H$. This fragment seems to contribute partly to stabilizing α-helix in the region 8–29 of bGHRF.

In conclusion we have shown, by NMR and molecular modeling, that full sequence of bGHRF adopts α-helix, β I(III)-turn and random conformation depending on the peptide region in 30% TFE mixed solvent solution. The β I(III)-turn region (residues 20–23) seems to be involved in the recognition site for affecting the receptor binding of bGHRF.

References

[1] Ling, N., Zeytin, F., Böhlen, P., Esch, F., Brazean, P., Wehrenberg, W.B., Baird, A. and Guillemin, R. (1985) Annu. Rev. Biochem. 54, 403–423.
[2] Noon, C. and Brook, C.G.D. (1985) Hosp. Update 11, 667–678.
[3] Lance, V.A., Murpy, W.A., Sueiras-Diaz, J. and Coy, D.H. (1984) Biochem. Biophys. Res. Commun. 119, 265–270.
[4] Coy, D., Murphy, W.A., Lance, V.A. and Heiman, M.L. (1987) J. Med. Chem. 30, 219–222.
[5] Tou, J.S., Kaempfe, L.A., Vineyard, B.D., Buonomo, F.B., Della-Fera, M.A. and Baile, C.A. (1986) Biochem. Biophys. Res. Commun. 139, 763–770.
[6] Esch, F., Bohlen, P., Ling, N., Guillemin, R. and Brazeau, P. (1983) Biochem. Biophys. Res. Commun. 117, 772–779.
[7] Clore, G.M., Martin, S.R. and Gronenborn, A.M. (1986) J. Mol. Biol. 191, 553–561.
[8] Brünger, A.T., Clore, G.M., Gronenborn, A.M. and Karplus, M. (1987) Protein Eng. 1, 399–406.
[9] Hocart, S.J., Murphy, W.A. and Coy, D.H. (1990) J. Med. Chem. 33, 1954–1958.
[10] River, J., Spiess, J. and Vale, W. (1982) Nature 303, 276–283.
[11] Wagner, G. and Wüthrich, K. (1982) J. Mol. Biol. 160, 343–361.
[12] Clore, G.M. and Gronenborn, A.M. (1985) J. Magn. Reson. 61, 158–164.
[13] Wüthrich, K. (1986) NMR of Proteins and Nucleic Acids, John Wiley and Sons, New York.
[14] Steward, J. and Young, J. (1984) Solid Phase Peptide Synthesis, 2nd Edn., Pierce Chem. Co., Rockford, IL.
[15] Chen, Y.H., Yang, T.Y. and Chan, K.M. (1974) Biochemistry 13, 3350–3359.
[16] SYBYL 6.3, Tripo, St. Louis, MO, USA.
[17] Güntert, P., Braun, W. and Wüthrich, K. (1991) J. Mol. Biol. 217, 517–530.
[18] Güntert, P. and Wüthrich, K. (1991) J. Biomol. NMR 1, 447–456.
[19] Widmer, H., Widmer, A. and Braun, W. (1993) J. Biomol. NMR 3, 307–324.
[20] King, G.F. and Mackay, J.P. (1996) in: Protein Structure Determination Using NMR Spectroscopy (Craik, D.J., Ed.), NMR in Drug Design, pp. 179–181, CRC Press, New York.
[21] Lee, M.S. and Cao, B. (1996) Protein Eng. 9, 15–25.
[22] Wishart, D.S., Sykes, B.D. and Richards, F.M. (1991) J. Mol. Biol. 222, 311–333.
[23] Clore, G.M., Gronenborn, A.M., Carson, G. and Mayer, E.F. (1986) J. Mol. Biol. 190, 259–267.
[24] Karplus, M. (1963) J. Am. Chem. Soc. 85, 2870–2871.
[25] Kessler, H., Mueller, A. and Oschkinat, H. (1985) Magn. Reson. Chem. 23, 844–852.
[26] Griesinger, C., Sorensen, O.W. and Ernst, R.R. (1987) J. Magn. Reson. 75, 462–474.
[27] Braun, W., Bösch, C., Brown, L.R., Gö, N. and Wüthrich, K. (1981) Biochim. Biophys. Acta 667, 377–396.
[28] Havel, T.F. and Wüthrich, K. (1984) Bull. Math. Biol. 46, 673–698.
[29] Nosaka, A.Y., Kanaori, K., Umemura, I., Takai, M. and Fujita, N. (1998) Bioorg. Med. Chem. 6, 465–472.
[30] Motta, A., Andreotti, G., Amodeo, P., Strazzullo, G. and Morelli, M. (1998) Proteins 32, 314–323.
[31] Möhle, K., Guβmann, M. and Hofmann, H.-J. (1997) J. Comp. Chem. 18, 1415–1430.
[32] Marshall, G.R. (1992) Curr. Opin. Struct. Biol. 2, 904–919.
[33] Gaudreau, P., Boulanger, L. and Abribat, T. (1992) J. Med. Chem. 35, 1864–1869.